Letter

Floquet time crystals as quantum sensors of ac fields

Fernando Iemini,[1,2] Rosario Fazio,[3,4] and Anna Sanpera[5,6]
[1]*Instituto de Física, Universidade Federal Fluminense, 24210-346 Niterói, Brazil*
[2]*Institute for Physics, Johannes Gutenberg University Mainz, D-55099 Mainz, Germany*
[3]*The Abdus Salam International Center for Theoretical Physics, Strada Costiera 11, I-34151 Trieste, Italy*
[4]*Dipartimento di Fisica "E. Pancini", Università di Napoli "Federico II", Monte S. Angelo, I-80126 Napoli, Italy*
[5]*Física Teòrica: Informació i Fenòmens Quàntics, Universitat Autònoma de Barcelona, E-08193 Bellaterra, Spain*
[6]*ICREA, Pg. Lluís Companys 23, E-08010 Barcelona, Spain*

(Received 15 June 2023; revised 10 January 2024; accepted 7 May 2024; published 30 May 2024)

The long-range spatial and temporal ordering displayed by discrete time crystals, can become advantageous properties when used for sensing extremely weak signals. Here, we investigate their performance as quantum sensors of weak ac fields and demonstrate, using the quantum Fisher information measure, that they can overcome the shot-noise limit while allowing long interrogation times. In such systems, collective interactions stabilize their dynamics against noise, making them robust enough to protocol imperfections.

DOI: 10.1103/PhysRevA.109.L050203

Introduction. Time crystals are nonequilibrium phases of matter that break time-translation invariance and present long-range time ordering. Originally proposed by Wilczek in isolated systems [1], it was soon realized that if energy is the only conserved quantity, time symmetry cannot be spontaneously broken in such cases [2]. Immediately after, several contributions demonstrated that time crystals may exist in out-of-equilibrium physics. Seminal theoretical investigations [3,4] put forward that periodically driven (Floquet) many-body interacting quantum systems can host time crystallinity, and its existence was soon after experimentally confirmed [5,6]. Since then, the field has become very active (see Refs. [7–10] and references therein for recent developments).

A Floquet time crystal (FTC) corresponds to a many-body interacting system driven by a periodic (Floquet) Hamiltonian of period T, i.e., $H(t) = H(t+T)$, that spontaneously breaks the *discrete* time-translation symmetry of the Hamiltonian. The FTC behavior can be probed by measuring an order parameter $O(t)$ (e.g., global spin magnetization) that displays subharmonic response, i.e., $O(t) = O(t+nT)$ ($n \in \mathbb{Z}; n > 1$). Crucially, such behavior is stable against Hamiltonian perturbations, defining a real quantum phase of matter.

Besides the relevance of FTCs in understanding the fundamental aspects of nonequilibrium quantum matter, time crystals may also offer advantages in applications. Investigations in this direction are, however, at an early stage [11–15]. In this Letter we make a step forward in this direction by exploring their potential as quantum sensors.

Interacting many-body quantum systems may act as precise sensors of different physical quantities, from electric and magnetic fields, to frequency and temperature among others [16]. Moreover, the quantum correlations present in the system may result in a quantum-enhanced sensitivity. Such enhancement is reflected in the so-called quantum Fisher information that bounds the minimal uncertainty with which an unknown parameter can be estimated, assuming one can optimize over all possible measurements. Furthermore, one can exploit the criticality of phase transitions, which enhances the correlation length of the system and its susceptibility to external fields [17,18], or alternatively use highly quantum entangled systems [e.g., Greenberger-Horne-Zeilinger (GHZ)-like states]. In such cases, the standard quantum limit (SQL) bounded by classical statistical correlations can be overcome, leading to the ultimate Heisenberg limit precision [19]. However, in nonequilibrium dynamics, entanglement heats up the system as well, leading inevitably to noise and instabilities that will deteriorating the sensor performance. Thus, sensors exploiting the entanglement resources present in many-body interacting systems, while having an exponentially slow heating, become robust to decoherence effects and are very promising for metrology.

Here, we use a spin system in a FTC phase as a quantum sensor of an ac field, and analyze its performance as a function of the properties of the FTC. Our approach takes a different route from the usual ones, which are mostly based on dynamical decoupling schemes [20–22], integrability [23], or prethermal stabilization of highly entangled states [24]. Before proceeding further let us briefly summarize our most relevant findings. The long-range spatial and time ordered dynamics present in the FTC, together with the presence of spin-spin correlations, allows for an optimal sensing performance for long times. Already for a moderate size of the sensor, its performance in time overcomes the standard quantum limit, even when estimating infinitesimal small ac fields. The breaking of the time-translational invariance is crucial for boosting the performance of the sensor. A generic Floquet system, with either ergodic or nonergodic dynamics, do not show similar advantages. Furthermore, FTCs can also be robust in the presence of dissipation [25] ensuring their capability as sensors.

The model. Our quantum sensor is composed of N spins described by the time-dependent Hamiltonian

$$\hat{H}_s = \sum_i \left[J_i \hat{\sigma}_i^z \hat{\sigma}_{i+1}^z + \sum_{\alpha=x,z} b_i^\alpha \hat{\sigma}_i^\alpha - \frac{\phi}{2} \sum_{n=-\infty}^{\infty} \delta(t - nT) \hat{\sigma}_i^x \right], \tag{1}$$

where $\hat{\sigma}_i^\alpha$ are Pauli operators at site i and component α. The system is subject to periodic kicks at intervals T, inducing a global ϕ rotation. Between the kicks, the system evolves under disordered interactions and fields, with disorder strengths, $J_i \in [1/2, 1/2 + J]$, $b_i^z \in [1/2, 1/2 + b^z]$, $b_i^x \in [0, b^x]$, chosen from a uniform distribution in the range of J, b^z, b^x. In the strong disordered regime and without kicking, the system evolves to a many-body localized (MBL) state, while the periodic kicking at $\phi \simeq \pi$ stabilizes a FTC phase [26] [see Supplemental Material (SM) [27] for details]. The system displays a period doubling in the magnetization dynamics as observed in several experiments [5,6,28–31].

The schematic of our protocol is shown in Figs. 1(a)–1(c); the sensor in the FTC phase is put in contact with an external ac field of amplitude h, and frequency ω_h along the z direction, coupling to the sensor through $\hat{V} = h \sin(\omega_h t + \theta) \sum_i \hat{\sigma}_i^z/2$. The sensor coupled to the external field evolves under the Hamiltonian $\hat{H}_s + \hat{V}$. We focus our discussions on estimating, with maximal accuracy, the amplitude field h, nevertheless, the analysis can be directly extended for the estimation of the associated frequency ω_h. In all our simulations we use initial separable states (see details in SM [27]), where we also discuss different initial states. We average our results over $n_{\rm dis} = 10^3$–10^4 disorder realizations, depending on the system size.

Optimal sensing can be reached once the period of the kicks in Eq. (1) is chosen to be $T \sim \pi/\omega_h$. In this case, the spins' dynamics is collectively phase locked with the ac field, allowing a long and coherent interrogation time. This is a unique trait of FTCs (not present in other nonergodic phases), and it is essential for the performance of the quantum sensor discussed here. Moreover, the presence of MBL dynamics due to the disorder leads to a growth of quantum correlations in the sensor boosting its performance. This is summarized schematically in Fig. 1(d), where the uncertainty in estimating h decreases with the duration of the sensing protocol. For the FTC sensor, such a decrease enhances its performance above the usual SQL, $[\Delta h(t)]_{\rm SQL} \propto t^{-1}$, displayed by either time-independent many-body Hamiltonians, or time-dependent ones after the transient regime. Furthermore, such an advantage lasts up to $\sim \max[t_{\rm th}, h^{-1}]$, where $t_{\rm th}$ is the thermalization time, which for the FTC sensor increases *exponentially* with its size N.

Sensing and quantum Fisher information. In the frequentist approach to sensing, typically, estimation protocols involve a repetition of the following steps: (i) the initialization of the sensor in an "advantageous/entangled" state; (ii) a time interval in which the sensor interacts with the signal of interest (in our case h), so that the unknown parameter is encoded in the state of the sensor; and (iii) a measurement on the quantum sensor. By collecting the statistics of the repeated protocol, one infers the value of the parameter with maximal

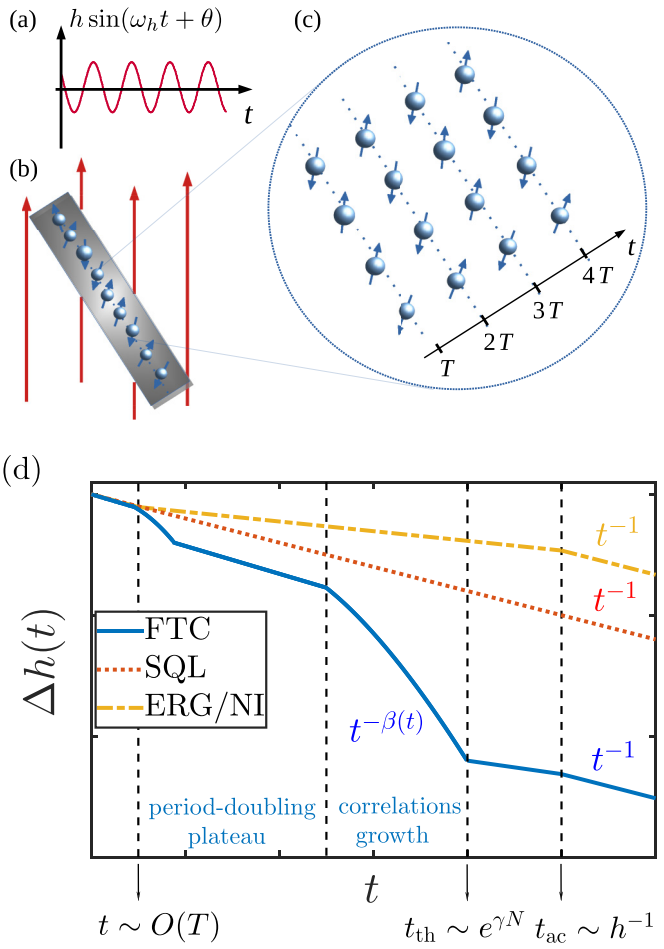

FIG. 1. Sketch of the FTC quantum sensor: (a) External ac field of amplitude h and frequency ω_h. (b), (c) The sensor is composed by N spins in a FTC, acting as a probe of the external ac field. (d) Variance for the optimal estimation of the amplitude $\Delta h(t)$ as a function of time for a generic ergodic or noninteracting phases (ERG/NI) and for a FTC phase. Due to its exponentially slow heating and many-body correlations, $\Delta h(t)$ in the FTC decreases faster than the SQL, $(\Delta h)_{\rm SQL} \sim 1/\sqrt{(2t/\pi)^2 N}$ (see Supplemental Material [27]) until thermalization times $t_{\rm th}$ are reached.

accuracy. Assuming that some prior knowledge of the parameter is known, the least uncertainty on the estimated parameter is settled by the quantum Cramér-Rao bound (details in SM [27]) $\Delta h(t) \geqslant 1/\sqrt{M F_h(t)}$ where $F_h(t)$ is the quantum Fisher information (QFI) of the probe and M is the number of measurements [32,33]. Notice that for an N many-body probe, the role of repeated measurements M can be played by N if the QFI is additive or can be superlinear in N if correlations are present. For pure states the QFI has the form

$$F_h(t)/4 = \langle \psi'(t,h)|\psi'(t,h)\rangle - |\langle \psi(t,h)|\psi'(t,h)\rangle|^2, \tag{2}$$

with $|\psi'(t,h)\rangle = \partial_h |\psi(t,h)\rangle$, the partial derivative with respect to the estimated parameter.

Case with $\phi = \pi$, $b_i^x = 0$, $h \to 0$. We consider perfect flips ($\phi = \pi$) during the kicks, no transverse magnetic fields, and the *linear-response* regime. In this case, one can obtain analytical results for the performance of the quantum sensor. Despite its simplicity, we can grasp several important properties of

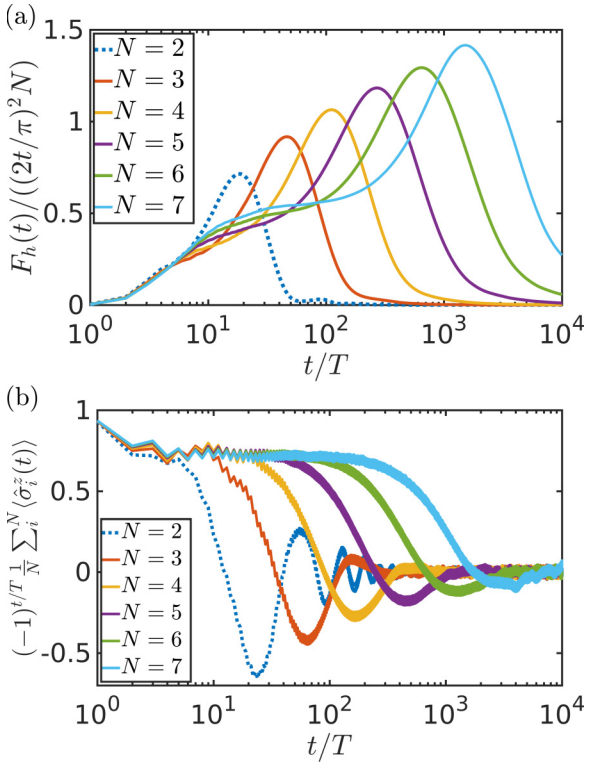

FIG. 2. (a) QFI dynamics as a function of the FTC sensor size N at resonance $\omega_h = \pi/T$. After an initial transient, the growth first saturates and then overcomes (due to the many-body correlations increase) the SQL [$F_h(t) \sim t^2$]. (b) The corresponding magnetization dynamics. The parameters here are set to $J = b^z = 0.25$, $b^x = 0.025$, $\theta = 0$, $\phi = 2.8$, $T = 1$, $\omega_h = \pi/T$, and $h \to 0$.

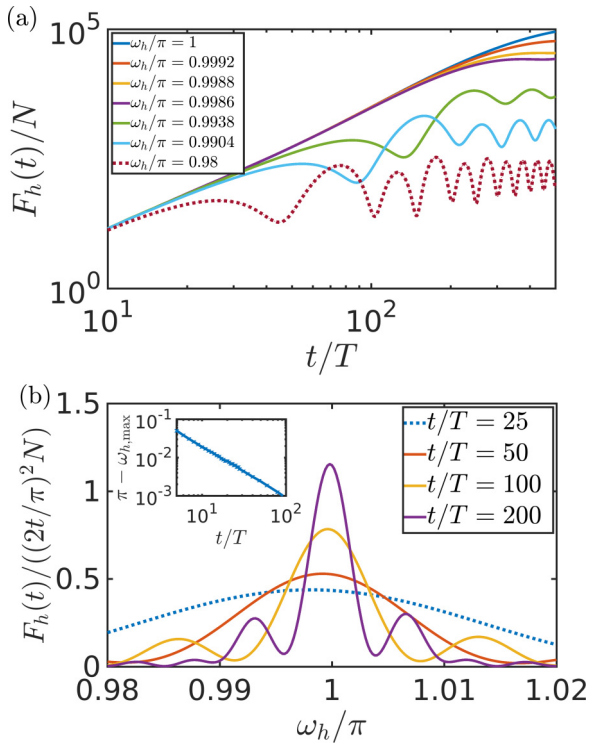

FIG. 3. Linear response for $N = 4$, and the same parameters as in Fig. 2, chosen to set the sensor in the FTC phase. (a) Dependence of the QFI dynamics with varying the ac frequency. (b) Frequency dependence of the QFI, at fixed times with a resonant peak emerging at long times. Inset: The position of the peak approaches the FTC frequency with increasing time.

the quality of the sensing protocol. The QFI reduces to (see SM [27])

$$F_{h\to 0}(t) = [\varphi(t)]^2 \,\mathrm{var}\left(\sum_i \hat{\sigma}_i^z\right). \tag{3}$$

Correlations among the spins, encoded in the variance of the total spin, may provide an enhanced sensing for the system (with a possible superlinear scaling with N). The time-dependent prefactor $\varphi(t) \equiv \int_0^t \sin(\omega_h t' + \theta)(-1)^{[t'/T]} dt'$ is the phase accumulated during the dynamics. This term is the same as for noninteracting sensing protocols, such as Carr-Purcell pulse trains [34] or periodic dynamical decoupling sequences [20]. The maximum accumulated phase (when the spin dynamics is in phase with the ac field) leads to a quadratic growth with time ($\sim t^2$). This happens when the spins are in resonance with the field, $T = \pi/\omega_h$, which for stroboscopic times $t = pT$ reduces to $\varphi(pT) \to (2pT/\pi)\cos\theta$ with p an integer number. Slight deviations $O(\epsilon)$ from the resonant case lead to off-resonance correction at timescales on the order of $t_{\rm off}/T = \theta/\epsilon$, for which the growth of the accumulated phase slows down. In order to see a scaling with an exponent $\beta > 1$ [see Fig. 1(d)], we have to consider the generic case discussed in the following.

General case. We now turn to the more realistic scenario, considering both imperfections in the kicks ($\phi \neq \pi$) as well as the presence of a transverse field, $b_i^x \neq 0$, that leads to decoherence in the dynamics. The interactions among the spins now strongly impact the dynamics of the system. In the resonant case ($T \sim \pi/\omega_h$), and in the linear-response regime, the dynamical behavior of the QFI is displayed in Fig. 2(a) for different sensor sizes N. In all cases, after an initial transient growth, the QFI first reaches a plateau, saturating the SQL growth in time ($\sim t^2$). At later times, the QFI overcomes the SQL due to correlation growth until the system thermalizes, at times exponentially divergent with N. In this intermediate regime, the maximum QFI has a higher than quadratic growth in time $F_h(t)/N \sim t^{2\beta(t)}$ with $\beta(t) > 1$. Similarly, the correlations along the ac field direction, quantified by the spin variance, shows an initial transient growth followed by a stable plateau, and a subsequent growth towards system thermalization (see SM [27]). The different regimes reflect the FCT dynamics, as shown in Fig. 2(b) for the total magnetization. After an initial transient time, $\mathcal{O}(T)$, it reaches a plateau whose lifetime corresponds to that of the QFI plateau. For longer times, dephasing due to MBL leads the magnetization to slowly decay towards its thermal value. The thermalization time (exponentially large in N) agrees with the time window for which the QFI overcomes the SQL scaling [i.e., the time when the QFI reaches its peak in Fig. 2(a)].

Indeed, Fig. 2 summarizes the potential of the FCT as a quantum sensor, beating the SQL for time intervals that scale exponentially with the size of the sensor.

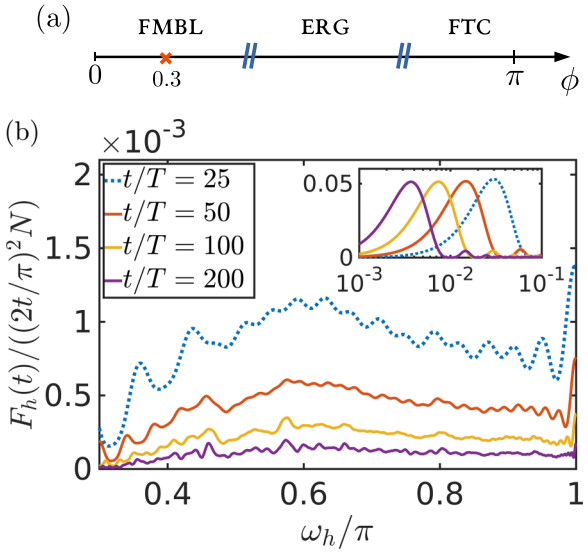

FIG. 4. (a) Schematic phase diagram of the sensor as a function of the global $\phi \in [0, \pi]$ rotation (induced from the periodic kicks), going from a Floquet MBL phase (FMBL), to an ergodic phase (ERG) and a Floquet time crystal (FTC). (b) The performance of the sensor in FMBL phase, displayed by the QFI, for parameters $\phi = 0.3$ (red cross in the schematic picture), $J = b^z = 0.25$, $b^x = 0.025$, $\theta = 0$, $T = 1$, and $N = 4$. The (noisy) response is upper bounded by the SQL. For decreasing frequencies $\omega_h \to 0$ (i.e., dc limit) the QFI displays the t^2 growth (peaks in the inset panel) due to the localization dynamics. The performance in the ergodic phase is similar to the FMBL case [27].

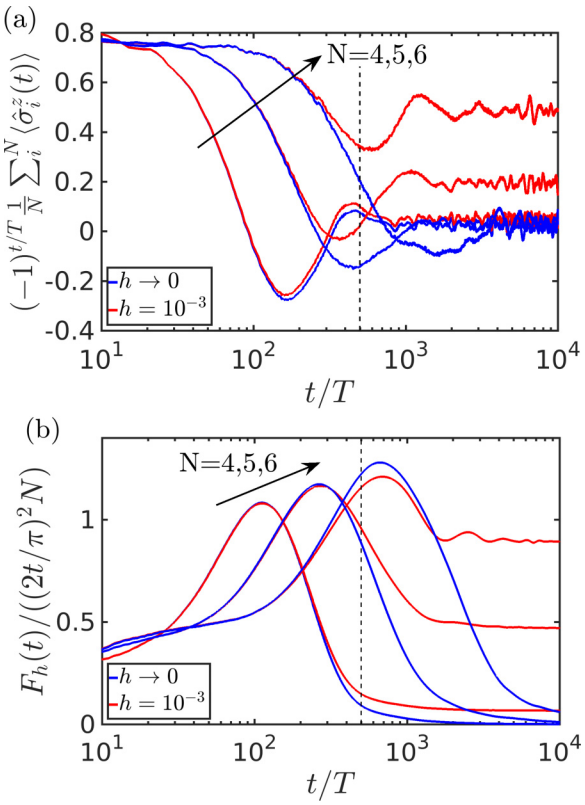

FIG. 5. Performance of the FTC sensor for finite field amplitudes h. The parameters are chosen to set the sensor in the FTC phase (same as in Fig. 2 but for varying h field). (a) Magnetization dynamics, with dominant ac effects appearing at timescales of the order of $t_{\rm ac} \sim h^{-1}$. (b) The QFI dynamics crosses over to a quadratic growth in time for $t \gtrsim t_{\rm ac}$. The vertical dotted line is a guide to the eye, setting the timescale $t_{\rm ac}$.

The optimal performance crucially depends on the tuning of the sensor frequency with the ac field, as shown in Figs. 3(a) and 3(b). Their mismatch sets a new characteristic time that scales with a power of the detuning. The response of the sensor to the ac field has nevertheless a well-structured form, as shown in Fig. 3(b). The collective interactions among the spins stabilize the sensor against noise.

As discussed previously, the performance of the FTC sensor can be enhanced by its initial preparation. For low-entangled initial states, similarly to the above case, there is var$(\sum_i \hat{\sigma}_i^z)$ factor that can lead to superextensive (with N) behavior. High-entangled GHZ-like initial states, known to be fragile to decoherence, show instead a different behavior with a continuous but very slow decay of the QFI dynamics—see SM [27]. In this case, despite the deterioration in performance, it is still attractive to exploit the sensor in a beneficial way due to such slow relaxation dynamics.

It is important to understand to which extent the properties of the sensor depend on the existence of the TC. This crucial point is reported in Fig. 4 where, by changing the global ϕ rotation, we can access to an MBL phase without time crystalline order, that we denote by FMBL, and to an ergordic phase (ERG), as schematically depicted in Fig. 4(a). The QFI in the FMBL phase is displayed in Fig. 4(b). Due to the absence of the phase-locked resonant features with the ac field, decisive for the performance of the sensor, the QFI in the FMBL can never beat nor reach the SQL. In the ergodic phase, the thermalization time is of the order of a few kicks, roughly independent on the system size. Also in this case, the QFI has no structured response to the probe field and its growth in time is always upper bounded by the SQL, as shown in SM [27].

Finally, we consider finite field amplitudes h, beyond linear response. The ac field becomes dominant for sufficiently long times and the sensor state is strongly influenced by the external field (therefore we expect a high sensibility for its estimation). Such effects appear at timescales of the order of $t_{\rm ac} \sim h^{-1}$. In the resonant case, the ac field tends to stabilize the period-doubling magnetization of the system, as shown in Fig. 5(a). In this regime the QFI ($t \gtrsim t_{\rm ac}$) shows a crossover to a purely quadratic growth in time [Fig. 5(b)], thus recovering the SQL. This behavior is apparently generic, i.e., independent on the sensor characteristics [27]. Therefore, one may interpret such a timescale $t_{\rm ac}$ as the strong ac field regime, where the detailed many-body properties of the sensor become unimportant for the measurement estimation. As in a linear response, off-resonant effects appear at times that scale with a power of the detuning, suppressing the period-doubling dynamics. The QFI slows down its growth recovering its quadratic growth. Also in this case, the QFI keeps its structured dependence with the probe, with a peak at resonance [27].

Conclusions. In this Letter we discuss FTCs as quantum sensors for ac fields. Their optimal performance—reached

once the sensor is set on period-doubling resonance to the field—is shown to offer several advantages, overcoming the shot-noise limit, allowing long-time sensing measurement times exponentially large with the number of spins, and being inherently robust to noise or imperfections in the protocol. Moreover, the sensor offers a promising dual role as a probe for unveiling the underlying ordering of the system in general cases. It would be interesting to explore other forms of time crystal sensors in closed (see, e.g., Refs. [35–40]) or in open systems with either discrete [41] or continuous [42,43] time-translation symmetry breaking.

Acknowledgments. F.I. acknowledges financial support from Alexander von Humboldt foundation and the Brazilian funding agencies CAPES, CNPQ, and FAPERJ (Grants No. 308205/2019-7, No. E-26/211.318/2019, No. 151064/2022-9, and No. E-26/201.365/2022), and by the Serrapilheira Institute (Grant No. Serra 2211-42166). A.S. acknowledges financial support from the Spanish Agencia Estatal de Investigacion, Grant No. PID2022-141283NB-I00, the European Commission QuantERA grant ExTRaQT (Spanish MICINN Project No. PCI2022-132965), by Ministerio de Ciencia e Innovación with funding from European Union NextGenerationEU (PRTR-C17.I1) and by Generalitat de Catalunya and the Spanish Ministry of Economic Affairs and Digital Transformation through the QUANTUM ENIA project call–Quantum Spain project, and the European Union through the Recovery, Transformation and Resilience Plan–NextGenerationEU within the framework of the Digital Spain 2025 Agend. R.F. acknowledges financial support from PNRR MUR Project No. PE0000023-NQSTI and by the European Union (ERC, RAVE, 101053159). The views and opinions expressed are however those of the author(s) only and do not necessarily reflect those of the European Union or the European Research Council. Neither the European Union nor the granting authority can be held responsible for them.

[1] F. Wilczek, Phys. Rev. Lett. **109**, 160401 (2012).
[2] H. Watanabe and M. Oshikawa, Phys. Rev. Lett. **114**, 251603 (2015).
[3] D. V. Else, B. Bauer, and C. Nayak, Phys. Rev. Lett. **117**, 090402 (2016).
[4] V. Khemani, A. Lazarides, R. Moessner, and S. L. Sondhi, Phys. Rev. Lett. **116**, 250401 (2016).
[5] S. Choi, J. Choi, R. Landig, G. Kucsko, H. Zhou, J. Isoya, F. Jelezko, S. Onoda, H. Sumiya, V. Khemani, C. von Keyserlingk, N. Y. Yao, E. Demler, and M. D. Lukin, Nature (London) **543**, 221 (2017).
[6] J. Zhang, P. W. Hess, A. Kyprianidis, P. Becker, A. Lee, J. Smith, G. Pagano, I.-D. Potirniche, A. C. Potter, A. Vishwanath, N. Y. Yao, and C. Monroe, Nature (London) **543**, 217 (2017).
[7] K. Sacha and J. Zakrzewski, Rep. Prog. Phys. **81**, 016401 (2018).
[8] D. V. Else, C. Monroe, C. Nayak, and N. Y. Yao, Annu. Rev. Condens. Matter Phys. **11**, 467 (2020).
[9] K. Sacha, *Time Crystals*, 1st ed. (Springer Nature, Cham, 2020).
[10] M. P. Zaletel, M. Lukin, C. Monroe, C. Nayak, F. Wilczek, and N. Y. Yao, Rev. Mod. Phys. **95**, 031001 (2023).
[11] M. P. Estarellas, T. Osada, V. M. Bastidas, B. Renoust, K. Sanaka, W. J. Munro, and K. Nemoto, Sci. Adv. **6**, eaay8892 (2020).
[12] R. W. Bomantara and J. Gong, Phys. Rev. Lett. **120**, 230405 (2018).
[13] F. Carollo, K. Brandner, and I. Lesanovsky, Phys. Rev. Lett. **125**, 240602 (2020).
[14] V. Montenegro, M. G. Genoni, A. Bayat, and M. G. A. Paris, Commun. Phys. **6**, 304 (2023).
[15] A. Cabot, F. Carollo, and I. Lesanovsky, Phys. Rev. Lett. **132**, 050801 (2024).
[16] C. L. Degen, F. Reinhard, and P. Cappellaro, Rev. Mod. Phys. **89**, 035002 (2017).
[17] P. Zanardi, M. G. A. Paris, and L. Campos Venuti, Phys. Rev. A **78**, 042105 (2008).
[18] C. Invernizzi, M. Korbman, L. C. Venuti, and M. G. A. Paris, Phys. Rev. A **78**, 042106 (2008).
[19] V. Giovannetti, S. Lloyd, and L. Maccone, Nat. Photon. **5**, 222 (2011).
[20] K. Khodjasteh and D. A. Lidar, Phys. Rev. Lett. **95**, 180501 (2005).
[21] D. Suter and G. A. Álvarez, Rev. Mod. Phys. **88**, 041001 (2016).
[22] H. Zhou, J. Choi, S. Choi, R. Landig, A. M. Douglas, J. Isoya, F. Jelezko, S. Onoda, H. Sumiya, P. Cappellaro, H. S. Knowles, H. Park, and M. D. Lukin, Phys. Rev. X **10**, 031003 (2020).
[23] U. Mishra and A. Bayat, Sci. Rep. **12**, 14760 (2022).
[24] N. Y. Y. Soonwon Choi and M. D. Lukin, arXiv:1801.00042.
[25] A. Riera-Campeny, M. Moreno-Cardoner, and A. Sanpera, Quantum **4**, 270 (2020).
[26] P. Sierant, M. Lewenstein, A. Scardicchio, and J. Zakrzewski, Phys. Rev. B **107**, 115132 (2023).
[27] See Supplemental Material at http://link.aps.org/supplemental/10.1103/PhysRevA.109.L050203 for further details on the QFI and the sensor sensor performance along the different phases of the model.
[28] J. Randall, C. E. Bradley, F. V. van der Gronden, A. Galicia, M. H. Abobeih, M. Markham, D. J. Twitchen, F. Machado, N. Y. Yao, and T. H. Taminiau, Science **374**, 1474 (2021).
[29] P. Frey and S. Rachel, Sci. Adv. **8**, eabm7652 (2022).
[30] X. Mi, M. Ippoliti, C. Quintana, A. Greene, Z. Chen, J. Gross, F. Arute, K. Arya, J. Atalaya, R. Babbush, J. C. Bardin, J. Basso, A. Bengtsson, A. Bilmes, A. Bourassa, L. Brill, M. Broughton, B. B. Buckley, D. A. Buell, B. Burkett *et al.*, Nature (London) **601**, 531 (2022).
[31] H. Xu, J. Zhang, J. Han, Z. Li, G. Xue, W. Liu, Y. Jin, and H. Yu, arXiv:2108.00942.
[32] S. L. Braunstein and C. M. Caves, Phys. Rev. Lett. **72**, 3439 (1994).
[33] J. Liu, H. Yuan, X.-M. Lu, and X. Wang, J. Phys. A: Math. Theor. **53**, 023001 (2020).
[34] H. Y. Carr and E. M. Purcell, Phys. Rev. **94**, 630 (1954).
[35] F. M. Surace, A. Russomanno, M. Dalmonte, A. Silva, R. Fazio, and F. Iemini, Phys. Rev. B **99**, 104303 (2019).

[36] K. Giergiel, A. Kosior, P. Hannaford, and K. Sacha, Phys. Rev. A **98**, 013613 (2018).
[37] P. Nurwantoro, R. W. Bomantara, and J. Gong, Phys. Rev. B **100**, 214311 (2019).
[38] K. Giergiel, T. Tran, A. Zaheer, A. Singh, A. Sidorov, K. Sacha, and P. Hannaford, New J. Phys. **22**, 085004 (2020).
[39] A. Pizzi, J. Knolle, and A. Nunnenkamp, Nat. Commun. **12**, 2341 (2021).
[40] G. Giachetti, A. Solfanelli, L. Correale, and N. Defenu, Phys. Rev. B **108**, L140102 (2023).
[41] Z. Gong, R. Hamazaki, and M. Ueda, Phys. Rev. Lett. **120**, 040404 (2018).
[42] F. Iemini, A. Russomanno, J. Keeling, M. Schirò, M. Dalmonte, and R. Fazio, Phys. Rev. Lett. **121**, 035301 (2018).
[43] B. Buča, J. Tindall, and D. Jaksch, Nat. Commun. **10**, 1730 (2019).